

**Cubosomes stabilized by a polyphosphoester-analog of Pluronic F127 with  
reduced cytotoxicity**

**DOI: 10.1016/j.jcis.2020.07.038**

*Marco Fornasier,<sup>a,b</sup> Stefania Biffi,<sup>c</sup> Barbara Bortot,<sup>c</sup> Paolo Macor,<sup>d</sup> Angelika  
Manhart,<sup>e</sup> Frederik R. Wurm,<sup>e,\*</sup> Sergio Murgia<sup>a,b,\*</sup>*

*<sup>a</sup>Department of Chemical and Geological Sciences, University of Cagliari, s.s. 554  
bivio Sestu, 09042 Monserrato, Cagliari, Italy.*

*<sup>b</sup>CSGI, Consorzio Interuniversitario per lo Sviluppo dei Sistemi a Grande Interfase, via  
della Lastruccia 3, 50019 Sesto Fiorentino, Florence, Italy.*

*<sup>c</sup>Institute for Maternal and Child Health, IRCCS Burlo Garofolo, Trieste, Italy.*

*<sup>d</sup>Department of Life Sciences, University of Trieste, Italy*

*<sup>e</sup>Max Planck Institute for Polymer Research, Ackermannweg 10, 55128 Mainz,  
Germany.*

## **Abstract**

Lyotropic liquid crystalline nanoparticles with bicontinuous cubic internal nanostructure, known as cubosomes, have been proposed as nanocarriers in various medical applications. However, as these nanoparticles show a certain degree of cytotoxicity, particularly against erythrocytes, their application in systemic administrations is limited to date. Intending to produce a more biocompatible formulation, we prepared cubosomes for the first time stabilized with a biodegradable polyphosphoester-analog of the commonly used Pluronic F127. The ABA-triblock copolymer poly(methyl ethylene phosphate)-block-poly(propylene oxide)-block-poly(methyl ethylene phosphate) (PMEP-*b*-PPO-*b*-PMEP) was prepared by organocatalyzed ring-opening polymerization of MEP. The cytotoxic features of the resulting formulation were investigated against two different cell lines (HEK-293 and HUVEC) and human red blood cells. The response of the complement system was also evaluated. Results proved the poly(phosphoester)-based formulation was significantly less toxic than that prepared using Pluronic F127 with respect to all the tested cell lines and, more importantly, hemolysis assay and complement system activation tests demonstrated its very high hemocompatibility. The potentially biodegradable poly(phosphoester)-based cubosomes represent a new and versatile platform for preparation of functional and smart nanocarriers.

**Keywords:** Lipid nanoparticles; nanomedicine; hemolysis; complement system

## 1. Introduction

In recent years, nanotechnologies provided an extraordinary boost to the chemistry of materials and, among the various fields in which they have been applied, nanomedicine is certainly one of the most investigated.[1] Possibly, the main result pursued by researchers working in this arena is the formulation of safe nanoparticles[2] able to precisely deliver drugs and/or imaging agents to pathological tissues, thus maximizing therapeutic effects while simultaneously reducing side effects, also in the perspective of personalized medicine. Yet, independently by all the efforts made so far, only a few nanomedicines have been translated from labs to market.[3,4] One of the reasons for such a negative outcome is the low biocompatibility of certain formulations. To overcome this limitation, formulations need to be engineered using safe building blocks. At the same time, it is necessary to provide nanoparticles with an appropriate surface coverage to avoid recognition from the Mononuclear Phagocyte System to extend their lifetime in the bloodstream.[5] In such a way, the desired therapeutic effect can be exerted at best keeping at minimum the dose of the drug, with the consequent reduction of adverse effects.

Cubosomes are soft nanoparticles characterized by a lyotropic liquid crystalline core prepared to exploit the natural self-assembly ability in water of several lipids (e.g., monoolein or phytantriol). They are often referred to as the non-lamellar analog of liposomes. Indeed, they are constituted by a three-dimensional, curved, and non-intersecting lipid double layer that, differently from liposomes, extends in space superimposed over an infinite periodic minimal surface of cubic symmetry, originating a network of two unconnected water channels.[6] Since they can host hydrophobic drugs and imaging probes, cubosomes are sometimes proposed as theranostic tools and, more in general, for application in the drug delivery field.[6–10] It is here worth

mentioning that cubosomes may host larger amounts of hydrophobic drugs with respect to liposomes, because they possess a larger hydrophobic (normalized) volume.[11] Cubosomes are traditionally prepared by fragmenting in water a liquid crystalline bicontinuous bulk phase by high-pressure homogenization or high-speed shearing (top-down approach) or by dissolving the lipids in water with the aid of a hydrotrope (bottom-up approach).[6] In both cases, a dispersant is generally added to the aqueous solution to stabilize the nanoparticles in water against flocculation. Generally, the used dispersant belongs to the family of non-ionic poly(ethylene oxide)–poly(propylene oxide)–poly(ethylene oxide) tri-block copolymers known as Pluronics, being the F127 the most representative. These copolymers interact with biological molecules of different kinds and are proposed as drug delivery carriers.[12–15] However, Pluronics are not biodegradable *in vivo* and activate the complement (which is part of the immune system) in the blood, they might cause cardiopulmonary distress in sensitive patients.[16] Other dispersant for the stabilization of cubosomes in water were less frequently reported in literature.[16–20] In some cases, it was found that the newly proposed stabilizers used as substitute of PF127 make the cubosome formulation less cytotoxic.[21,22]

Here, we present novel cubosomes with improved biocompatibility and the potential to be fully biodegradable by the use of an amphiphilic poly(phosphoester) (PPE) analog of Pluronic F127 (PF127). PPEs are polyesters, based on phosphoric acid derivatives that possess the remarkable characteristic of being highly stable but also degradable on demand.[23,24] Especially synthetic PPEs have been studied by Wurm's group intensely as alternatives for poly(ethylene glycol) in drug delivery applications.[25] This article presents detailed physicochemical and cytotoxic analyses of PPE-based cubosomes and compared them with traditional cubosomes stabilized by PF127, to

assess their possible application as biodegradable drug delivery system. With the chemical versatility of PPEs, this strategy opens a new platform for the design of bicontinuous cubic liquid crystalline nanoparticles with additional chemical functionality and a controlled degradation pattern.

## **2. Materials and Methods**

### *2.1 Materials*

The main component of the cubosomes, glycerol monooleate (MO, 1-monooleoylglycerol, RYLO MG 19 PHARMA, 98.1 wt%) was kindly provided by Danisco A/S (Denmark). Sodium citrate dihydrate (99.0 %), citric acid (99.9 %), sodium dihydrogen phosphate (99.9 %), sodium hydrogen phosphate (99.9 %), sodium chloride (99.9 %), potassium chloride (99.9 %), and quercetin ( $\geq 95.0$  %) were purchased from Sigma-Aldrich. Fresh distilled water purified using a Milli-Q system (Millipore) was used for preparing each sample and it was filtered with a 0.22  $\mu\text{m}$  pore size hydrophilic filter prior to any use.

The Human Embryonic Kidney 293 (HEK-293) and the Human Umbilical vein/vascular endothelium (HUVEC) cell lines were purchased from ATCC (American Type Culture Collection, Manassas, Virginia United States). The CellTox™ Green Cytotoxicity Assay kit and the Apo-ONE® Homogeneous Caspase-3/7 Assay kit were purchased from Promega (Madison, WI). For fluorescence microscopy cells were stained with MitoTracker® Red CMXRos and Weat Germ Agglutinin (WEG) Conjugates Alexa Fluor® 350 conjugate (Invitrogen, Thermo Fischer Scientific, Waltham, Massachusetts, USA).

$^1\text{H}$  and  $^{31}\text{P}$  Nuclear Magnetic Resonance Spectroscopy. For nuclear magnetic resonance (NMR) analyses,  $^1\text{H}$  and  $^{31}\text{P}$  NMR spectra were recorded on a Bruker AVANCE III 500 spectrometer operating with 500 MHz and 202 MHz frequencies, respectively.

Size Exclusion Chromatography. Size exclusion chromatography (SEC) measurements were performed in DMF containing  $0.25\text{ g L}^{-1}$  of lithium bromide at  $50\text{ }^\circ\text{C}$  and a flow rate of  $1\text{ mL min}^{-1}$  with an Agilent 1100 Series as an integrated instrument, including a PSS HEMA column ( $106/105/104\text{ g mol}^{-1}$ ), a UV (275 nm) and a refractive index (RI) detector. Calibration was carried out using poly(ethylene glycol) standards provided by Polymer Standards Service.

## 2.2 Polyphosphoester synthesis

Monomer Synthesis: *2-Methoxy-2-oxo-1,3,2-dioxaphospholane (MEP)*. A flame-dried 1000 mL three-neck flask, equipped with a dropping funnel, was charged with 2-chloro-2-oxo-1,3,2-dioxaphospholane (50 g, 0.35 mol) dissolved in dry THF (300 mL). A solution of dry methanol (11.24 g, 0.35 mol) and dry pyridine (27.72 g, 0.35 mol) in dry THF (45 mL) was added dropwise to the stirring solution of COP at  $-20\text{ }^\circ\text{C}$  under argon atmosphere. During the reaction, hydrogen chloride was formed and precipitated as pyridinium hydrochloride. The reaction was stirred at  $4\text{ }^\circ\text{C}$  overnight. The salt was removed by filtration and the filtrate concentrated *in vacuo*. The residue was purified by distillation at reduced pressure to give a fraction at  $89\text{--}97\text{ }^\circ\text{C}/0.001\text{ mbar}$ , obtaining the clear, colorless, liquid product MEP (25.54 g, 0.19 mol, yield: 53%).  $^1\text{H-NMR}$  (500 MHz,  $\text{DMSO-d}_6$ ):  $\delta$  4.43 (m, 4H), 3.71 (d, 3H).  $^{13}\text{C}\{^1\text{H}\}$  NMR (125 MHz,  $\text{DMSO-d}_6$ ):  $\delta$  66.57, 54.72.  $^{31}\text{P}\{^1\text{H}\}$  NMR (202 MHz,  $\text{DMSO-d}_6$ ):  $\delta$  17.89.

*Polymerization of MEP.* *N*-cyclohexyl-*N'*-(3,5-bis(trifluoromethyl)phenyl)thiourea (TU) was synthesized according to the literature procedure.[26] TU (268 mg,  $7.2 \cdot 10^{-4}$  mol) and the poly(propylene oxide)<sub>68</sub>-macroinitiator (75  $\mu$ mol, 300 mg, PPO-diol of molar mass  $4,000 \text{ g mol}^{-1}$  was used) were placed in a Schlenk tube and freeze-dried with benzene prior use. 5 mL of dry dichloromethane and freshly distilled MEP (1.83 g,  $15 \cdot 10^{-3}$  mol) were added to the mixture. The solution was cooled down to 0 °C, then the polymerization was initiated by the rapid addition of 0.12 mL DBU (113 mg,  $7.2 \cdot 10^{-4}$  mol) to the stirred solution. The polymerization was terminated after 90 min by the addition of ca. 1 mL acetic acid in dichloromethane ( $1 \text{ mol L}^{-1}$ ). The polymer was purified by precipitation from dichloromethane into ice-cold ethyl acetate twice and finally into ice-cold diethyl ether, followed by dialysis against deionized water overnight (MWCO: 3500). The polymer was obtained after freeze-drying in quantitative yield.

### *2.3 Pendant Drop Surface Tension measurements*

The PPE surface tension was measured using a tensiometer (Sinterface Technologies, Germany) equipped with a recording camera, from the shape of a pendant drop of  $20 \text{ mm}^3$  at different concentrations of the polymer in an aqueous solution (in the range 0.01 – 180  $\mu$ M). The shape was obtained using the Gauss-Laplace equation, a relationship between the curvature of a liquid meniscus and the surface tension,  $\gamma$ , that can be determined by the Gauss-Laplace equation to the coordinates of a drop. The fitting was performed using the PAT fitting software. The surface tension for each concentration was measured after 8000 s of equilibrium time at least.

#### 2.4 Cubosome formulation

To obtain the cubosomes formulation, at first, MO was melted at 40 °C (drug loaded cubosomes were prepared by adding quercetin to the melted MO). A clear solution of PPE polymer was then added to the lipid phase and the mixture was ultrasonicated usually for 2 cycles of 5 min (Amplitude 40 %, 1 s ON and 1 s OFF) using a tip-sonicator equipped with a controller Sonics Vibra Cells, both from Chemical Instruments AB (Sweden). Cubosomes formulations here investigated had the following composition in wt % (the name of the corresponding sample is in parenthesis): MO/PF127/Water = 3.3/0.3/96.4 (Cubo-0.3F127) and MO/PPE/Water = 3.3/0.3/96.4, 3.3/0.6/96.1, 3.3/0.9/95.8, 3.3/1.2/95.5 (Cubo-0.3PPE, Cubo-0.6PPE, Cubo-0.9PPE, and Cubo-1.2PPE, respectively).

#### 2.5 Encapsulation efficiency

After loading with quercetin, formulations Cubo-0.3F127 and Cubo-0.6PPE were dialyzed into a tubing cellulose membrane (14 kDa molecular weight cutoff, purchased from Sigma Aldrich) against 2 L of water at room temperature for 2 hours (water was changed after 1 hour). The adsorption spectra of quercetin ( $\lambda_{\text{abs}} = 373 \text{ nm}$ ) were acquired using a Win-Cary Varian UV-Vis double-beam spectrophotometer in EtOH. A standard calibration curve was built up to evaluate the loading of the antioxidant adopting a linear regression analysis (correlation coefficient,  $R^2 = 0.9999$ ). The quercetin-loaded formulations (before and after dialysis) were then dissolved in EtOH and placed in quartz cuvette (1 cm of optical path). The encapsulation efficiency (%) of quercetin into the formulation was calculated exploiting the following expression:

$$EE(\%) = \frac{\text{mass of drug after dialysis}}{\text{mass of drug before dialysis}} \cdot 100$$



## *2.6 Dynamic Light Scattering and Electrophoretic Mobility experiments*

The cubosome formulations were diluted 1:50 in water at least 24 h after preparation and before any measurement. The mean nanoparticles size (diameters) was characterized employing Dynamic Light Scattering (size and polydispersity index, Pdl) and Electrophoretic Mobility ( $\zeta$ -potential), using a ZetaSizer Nano ZS by Malvern Instruments (Malvern, UK) at  $(25.0 \pm 0.1)$  °C (backscattering angle 173°, 4 mW He-Ne laser at 663 nm). Size, Pdl, and  $\zeta$ -potential of each sample was collected at least 5-6 times. The stability of the formulations was also evaluated measuring these parameters up to five months while keeping the samples at 25 °C. The formulation Cubo-0.6PPE was studied at two different pHs (3.4 and 7.4) by diluting the dispersion prepared in water into the desired buffer 1:50 before performing the DLS and  $\zeta$ -potential measurements.

## *2.7 Electron Microscopy at cryogenic temperature (cryo-TEM)*

The cubosomes were imaged by cryo-TEM, using a JEM-2200FS transmission electron microscope (JEOL), optimized for cryo-TEM at the National Center for High Resolution Electron Microscopy (nCHREM) at Lund University. The instrument is equipped with a field-emission electron source, a cryo pole piece in the objective lens and an in-column energy filter (omega filter). Zero-loss images were recorded at an acceleration voltage of 200 kV on a bottom-mounted TemCam-F416 camera (TVIPS) using SerialEM under low-dose conditions. Each sample was prepared using an automatic plunge freezer system (Leica Em GP) with the environmental chamber operating at 25.0 °C and 90 % of relative humidity. A 4  $\mu$ L droplet of the cubosomes formulation was deposited on a lacey formvar carbon-coated grid (Ted Pella) and was

blotted with filter paper to remove excess fluid. The grid was then plunged into liquid ethane (around  $-183\text{ }^{\circ}\text{C}$ ) to ensure the rapid vitrification of the sample in its native state. The specimens were thereafter stored in liquid nitrogen ( $-196\text{ }^{\circ}\text{C}$ ) and before imaging transferred into the microscope using a cryo transfer tomography holder (Fischione, Model 2550).

### 2.8 Small Angle X-ray Scattering (SAXS)

SAXS experiments were performed at the SAXSLab instrument (JJ-Xray, Denmark) at Lund University equipped with a 30 W Cu X-RAY TUBE for GeniX 3D and a 2D 300 K Pilatus detector (Dectris). The measurements were acquired with a pin-hole collimated beam with the detector positioned asymmetrically to yield a single measurement  $q$ -range of  $0.012 - 0.67\text{ }\text{\AA}^{-1}$ . The sample-to-detector distance was 480 mm in all experiments.

The magnitude of the scattering vector is defined by  $q = (4\pi \sin\theta)/\lambda$ , where  $\lambda$  equals to  $1.54\text{ }\text{\AA}$ , Cu  $K\alpha$  wavelength, and  $\theta$  is half of the scattering angle. The  $d$  spacing was calculated using the following expression:

$$d = \frac{2\pi}{q} \quad (\text{eq. 1})$$

Then, the lattice parameter,  $a$ , was obtained by eq. 2 and eq. 3 for the bicontinuous cubic and hexagonal phases, respectively.

$$a = d \cdot \sqrt{h^2 + k^2 + l^2} \quad (\text{eq. 2})$$

$$a = d \cdot \frac{2}{\sqrt{3}} \sqrt{h^2 + k^2 + hk} \quad (\text{eq. 3})$$

Here,  $h$ ,  $k$  and  $l$  are the Miller indexes that describe the crystalline planes. The values of  $a$  were also used to calculate the water channel radius ( $r_w$ ) of the bicontinuous cubic phase (eq. 4) or of the hexagonal phase (eq. 5):

$$r_w = \sqrt{\frac{A_0}{-2\pi}} \cdot a - l \quad (\text{eq. 4})$$

$$r_w = a \cdot \sqrt{1 - \varphi_{lipid}} \cdot \left(\frac{\sqrt{3}}{2\pi}\right)^{\frac{1}{2}} \quad (\text{eq. 5})$$

where  $\chi$  and  $A_0$  are, respectively, the Euler characteristic and the surface area of the IPMS geometry (Pn3m,  $\chi = -2$ ,  $A_0 = 1.919$ ), and  $l$  is the MO hydrophobic chain length at 25 °C (17 Å). The lipid fraction,  $\varphi_{lipid}$ , was calculated using the following equation (eq. 6), where  $w_{MO}$ ,  $d_{MO}$ ,  $w_{water}$  and  $d_{water}$  are the weight and density of MO and water respectively:

$$\varphi_{lipid} = \frac{\frac{w_{MO}}{d_{MO}}}{\left(\frac{w_{MO}}{d_{MO}} + \frac{w_{water}}{d_{water}}\right)} \quad (\text{eq.6})$$

The temperature in the analysis chamber was controlled using a Julabo T Controller CF41 from Julabo Labortechnik GmbH (Germany). The T range measurements were acquired after equilibrating the sample for 1 h at the given temperature.

The angular scale was calibrated using silver behenate,  $\text{CH}_3\text{-(CH}_2\text{)}_{20}\text{-COOAg}$ , as a standard.

To evaluate the effect of the pH on the formulation Cubo-0.6PPE, few drops of the buffer (citrate or PBS) were added to the cubosomes dispersion until the target pH was reached. The mixture was then let equilibrate for 30 min prior to any measurements.

### *2.9 Cytotoxicity and apoptosis assays*

HEK cells were grown in DMEM medium (Euroclone, Milan, Italy) supplemented with 10% fetal bovine serum (Euroclone, Milan, Italy) and 1% penicillin/streptomycin antibiotics (Euroclone, Milan, Italy) at 37°C in a humidified incubator with 5% CO<sub>2</sub>. HUVEC cells were maintained in F-12K medium, adding appropriate components, as recommended by the manufacturer. HEK-293 and HUVEC cells were seeded at a density of  $5 \times 10^4$  cells/well in 96-multiwell plate (Corning, New York, USA). After 24 hours, formulations Cubo-0.3F127 and Cubo-0.6PPE were added in the culture medium at MO concentrations of 10, 25, 50, 75, 100 µg/mL. After 24, 48 and 72 h of incubation, CellTox™ Green Cytotoxicity Assay kit (Promega Madison, WI) was used to quantify cytotoxicity, and Apo-ONE® Homogeneous Caspase-3/7 Assay kit (Promega Madison, WI) was used to determine caspase-3/7 activity according to the manufacturer's instructions. The fluorescence was determined by GloMax® Discover Microplate Reader instrument (Promega Madison, WI). All data collected are reported as the mean and standard deviation of three independent experiments.

### *2.10 Hemolysis assay*

Red blood cells were freshly isolated and analyzed as previously reported.[27] The whole blood sample was freshly obtained from the experimenter (female healthy volunteer, SB) upon written informed consent. Briefly, the erythrocytes were separated from the whole blood by centrifugation at 1500 rpm for 10 min, washed three times,

and diluted with saline solution (0.9% NaCl). 50 mL of the erythrocyte stock dispersion was added to 950 mL of saline containing different concentrations of formulations Cubo-0.3F127 and Cubo-0.6PPE (MO concentrations of 10, 25, 50, 75, 100 µg/mL). Saline solution (0.9% NaCl) and distilled water were employed respectively as the negative control (0 % lysis) and positive control (100 % lysis). After 1 hour of incubation, the absorbance of the supernatant separated upon centrifugation at 10 000 rpm for 5 min was recorded at 560 nm UV-vis using GloMax® Discover Microplate Reader instrument (Promega Madison, WI).

### *2.11 Complement activity assay*

Human serum (0.1 mL) was incubated with or without Cubo-0.3F127 or Cubo-0.6PPE (see section 2.4) at the final concentration of 660 µg/mL for 2 h at 37 °C; at the end, the reaction was blocked adding EDTA at the final concentration of 20 mM. The residual hemolytic activity of the classical pathway of the C system was then evaluated incubating different dilution (1:50, 1:100, 1:200, 1:400) of treated human serum with IgM-sensitized sheep red blood cells (50 mL at  $1.5 \times 10^7$ ) in glucose veronal-buffered saline for 30 minutes at 37 °C; hemoglobin released from lysed red blood cells was evaluated reading the supernatant after centrifugation at 415 nm.[28]

### *2.12 Cell fluorescence imaging*

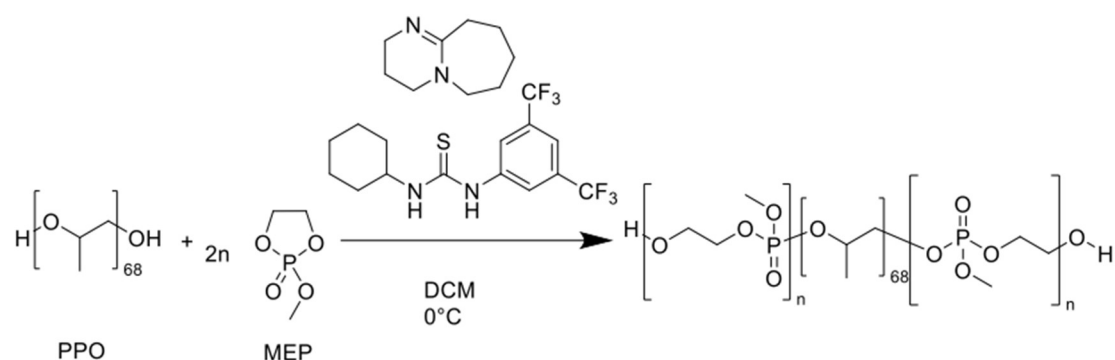
HUVEC cells were seeded in slides (20x20) coated with 50 µg/mL human fibronectin (Corning, New York, USA) at a density of  $2.5 \times 10^5$  onto 6-well plate (Corning, New York, USA). Cells were incubated for 24 h in medium alone (control) or in presence of formulations Cubo-0.3F127 or Cubo-0.6PPE at the MO concentration of 100 µg/mL. Wheat Germ Agglutinin Conjugates Alexa Fluor® 350 conjugate was used at a

concentration of 5  $\mu\text{g/mL}$  at 37  $^{\circ}\text{C}$  for 20 minutes to stain cell membranes. MitoTracker<sup>®</sup> Red CMXRos probe was used at a concentration of 200 nM at 37  $^{\circ}\text{C}$  for 20 minutes to reveal the mitochondria distribution. Cells were washed twice with D-PBS buffer (Euroclone, Milan, Italy) and fixed with paraformaldehyde (PFA) 4% (MERCK, Darmstadt Germania) for 30 minutes. The slides were mounted using Vectashield mounting medium for fluorescence with DAPI (Vector Laboratories Inc. Burlingame, CA) to stain cellular nuclei. Fluorescent images of cells were acquired by using an inverted microscope with a CCD camera, and the objectives lens 20X (Axioplan2, with Axiocam MRc, ZEISS Oberkochen Germany).

### 3. Results and discussion

#### 3.1 Poly(phosphoester) synthesis

For the preparation of a PPE-based pluronic mimic, we used poly(propylene oxide)<sub>68</sub> (with a molar mass of 4,000 g/mol) as a difunctional initiator for the organocatalyzed ring-opening polymerization of MEP (Scheme 1 and Experimental for details).



Scheme 1: Synthesis of  $\text{PMEP}_{105}\text{-}b\text{-PPO}_{68}\text{-}b\text{-PMEP}_{105}$  triblock copolymer by organocatalyzed ring-opening polymerization.

TU and DBU were used as the organocatalytic system and a PPE polymer with the composition  $\text{PMEP}_{105}\text{-}b\text{-PPO}_{68}\text{-}b\text{-PMEP}_{105}$  ( $M_n = 33,000$  g/mol – from  $^1\text{H}$  NMR) was

obtained. The degree of polymerization of MEP was determined from the  $^1\text{H}$  NMR spectrum (Figure S1) by comparing the resonances of the PPO macroinitiator at 1.1 ppm (methyl side chain) with the doublet of the methoxy side chains of PMEPE at 3.8 ppm. SEC molar masses were strongly underestimated with  $M_n = 3500$  g/mol (vs. PEG standards, as reported previously for similar polymers on our setup) but a monomodal molar mass distribution with a dispersity  $D = 1.4$  (from SEC in DMF) was determined. The critical micelle concentration (CMC) of the PPE in water was extrapolated from a series of measurements at increasing concentration of the polymer using a pendant-drop tensiometer. From the Gauss-Laplace fitting a CMC value of  $1.92$   $\mu\text{M}$  was obtained.

### *3.2 Cubosome characterization*

The cubosome formulations here investigated were prepared by dispersing the molten MO in an aqueous dispersion of PF127 (Cubo-0.3F127) or the newly synthesized PPE (Cubo-0.3PPE, Cubo-0.6PPE, Cubo-0.9PPE, and Cubo-1.2PPE), as described in Section 2.4. The PPE was used as a stabilizing agent for the nanoparticles in substitution of the commonly used PF127. To verify the possibility of forming cubosomes using the PPE, investigate its stabilizing properties, and observe if and how it could alter the morphology and the topology of these nanoparticles, different samples were prepared at increasing concentration of PPE (from 0.3 to 1.2 wt%, see Section 2.4). The macroscopic appearance of all the samples was that of milky, highly fluid aqueous solutions as typically observed for this kind of formulations. The presence of cubosomes was proven by cryo-TEM and SAXS experiments.

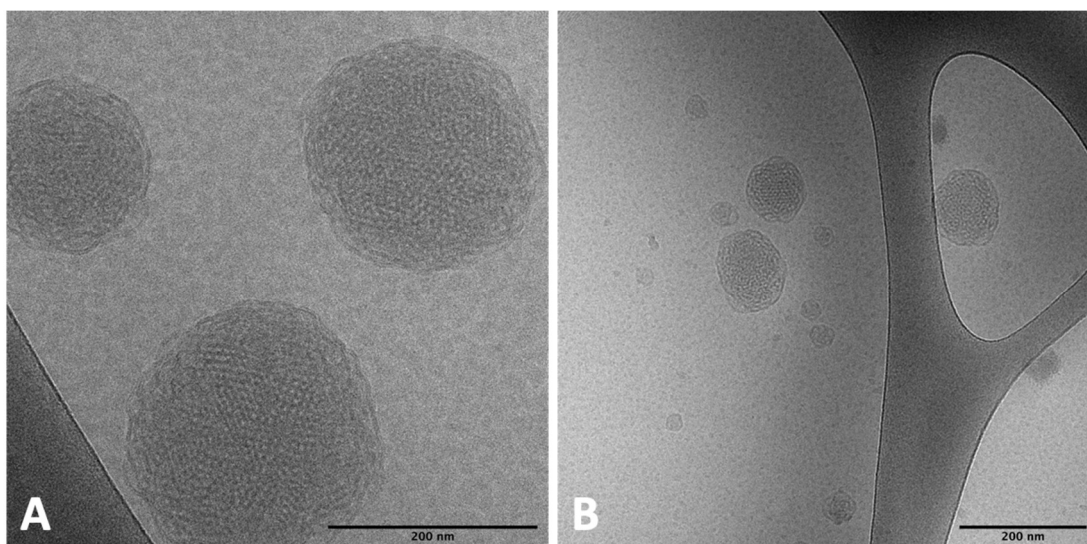


**Figure 1.** Cryo-TEM images of formulations Cubo-0.6PPE (A) and Cubo-1.2PPE (B).

In Figure 1 are reported the cryo-TEM images of samples Cubo-0.6PPE and Cubo-1.2PPE, emblematic for all the formulations stabilized by the PPE. As can be seen, they consisted in aqueous dispersions of spherical nanoparticles exhibiting a dense inner matrix characterized by a honeycomb structure. It is worth noticing that, although cubosomes appeared as nanoparticles having cubic morphology in numerous scientific articles, they were also often observed as round shaped, as in the present case. In Figure 1B it can be also noticed the presence of small objects presenting the so-called interlamellar attachments, which are considered intermediates in the transition from lamellar to reverse bicontinuous cubic structures.[29] Remarkably, cryo-TEM images did not show the presence of the small unilamellar vesicles (SUVs) usually found in coexistence with cubosome nanoparticles stabilized by PF127 (see also Figure S2). Since MO does not form SUVs in excess of water, the existence of these aggregates can be attributed to the presence of the stabilizing agent. In turn, the observed absence of SUVs in the samples here under investigation may suggest a different type of interaction among the PPE and MO with respect to PF127. The topology of the



nanoparticles' inner core was assessed by SAXS. The diffraction patterns reported in Figure 2 revealed that nanoparticles in formulations Cubo-0.3PPE to Cubo-1.2PPE were constituted by a pure Pn3m bicontinuous cubic phase, while formulation Cubo-0.3F127 was characterized by the coexistence of both the Pn3m and the Im3m phases.

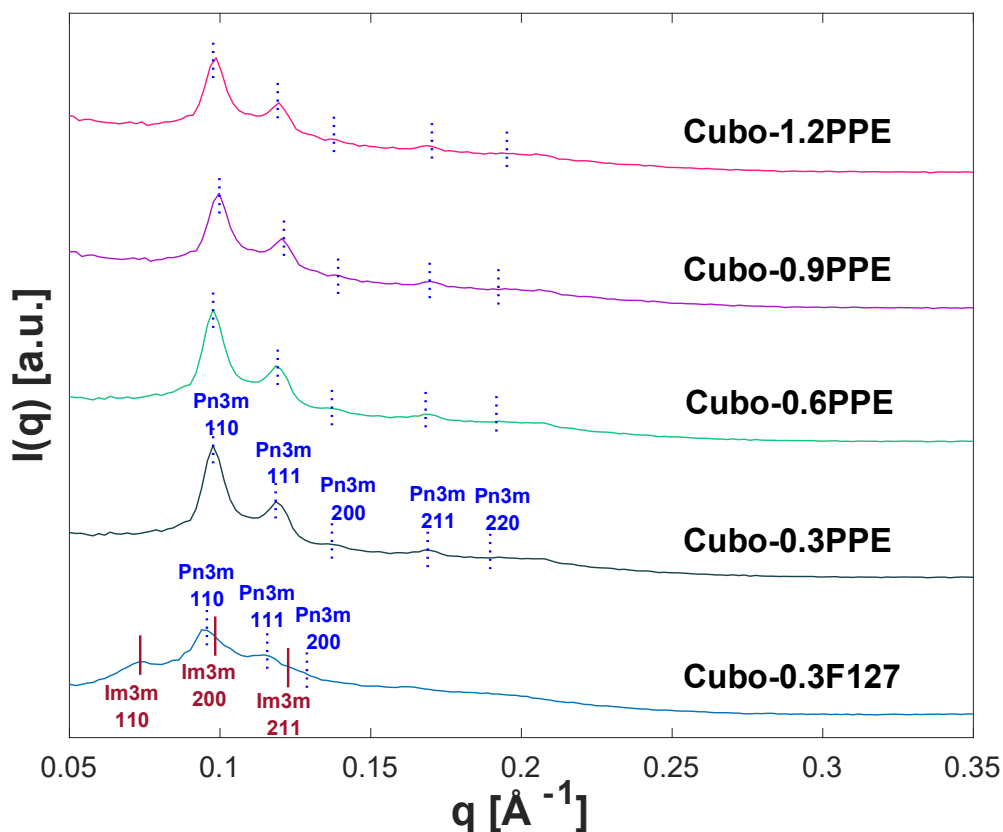


**Figure 2.** SAXS diffractograms at 25 °C of the investigated cubosomes formulations. On the top of the corresponding Bragg peaks, the Miller indices are also reported along with the indication of the phase. Formulation Cubo-0.3F127 was stabilized using Pluronic F127, while formulations Cubo-0.3PPE to Cubo-1.2PPE were stabilized using increasing concentrations of the newly synthesized PPE polymer (see also Section 2.4).

Pioneering SAXS experiments on cubosomes by Nakano *et al.* demonstrated that interaction of the poly-(propylene oxide) block of P127 with the nanoparticle internal

bicontinuous cubic phase causes a Pn3m-to-Im3m inter-cubic phase transition.[30] While the PPE shares the same hydrophobic block of PF127, no Bragg peaks belonging to other phases different from the Pn3m can be observed in all the formulations stabilized with the PPE here investigated. This finding strongly suggests that the hydrophilic arms of the stabilizing polymer may have a role in the inter-cubic phase transition process and reinforce the idea that the PPE interacts with MO aggregates differently from PF127. From data reported in Table 1, it can be also observed that the Pn3m phase characterizing the cubosomes has a slightly smaller lattice parameter, 91.2 Å rather than 95.8 Å, when PPE is used to replace PF127 as stabilizer. However, the tiny variation of the observed lattice parameter while varying the PPE content along the Cubo-0.3PPE, Cubo-0.6PPE, Cubo-0.9PPE, and Cubo-1.2PPE sample series is very close to the experimental error and it seems not significant. Moreover, the presence of the PPE into the formulation influences slightly the lattice parameters of the Pn3m phase in comparison with cubosomes stabilized by PF127 (Table 1).

**Table 1.** Phase, lattice parameter ( $a$ ), water channel radius ( $r_w$ ), average diameter of the nanoparticles ( $D$ ), polydispersity index (PdI), and  $\zeta$ -potential of all the cubosomes formulations investigated at 25 °C. Data are reported as mean  $\pm$  SD.

Sample	Phase	$a$ (Å)	$r_w$ (Å)	$D$ (nm)	PdI	$\zeta$ -potential (mV)
Cubo-0.3F127	Pn3m	95.8 $\pm$ 0.8	20.4 $\pm$ 0.5	141 $\pm$ 1	0.11 $\pm$	- 25 $\pm$ 1
	Im3m	126.4 $\pm$ 0.6	21.8 $\pm$ 0.5		0.02	
Cubo-0.3PPE	Pn3m	92.6 $\pm$ 0.5	19.2 $\pm$ 0.1	200 $\pm$ 3	0.23 $\pm$ 0.01	- 45 $\pm$ 1

Cubo-0.6PPE	Pn3m	91.2 ± 0.6	18.6 ± 0.1	160 ± 1	0.09 ± 0.01	- 47 ± 1
Cubo-0.9PPE	Pn3m	90.7 ± 0.5	18.4 ± 0.1	148 ± 1	0.12 ± 0.02	- 51 ± 2
Cubo-1.2PPE	Pn3m	90.8 ± 0.4	18.5 ± 0.1	143 ± 2	0.11 ± 0.02	- 48 ± 2

As reported in Table 1, DLS experiments showed that increasing amounts of the PPE lead to smaller nanoparticles with low polydispersity index, and that all the formulations were characterized by a high negative  $\zeta$ -potential (around  $-50$  mV), much larger than that recorded for the formulation Cubo-0.3F127. The origin of the negative  $\zeta$ -potential sometimes observed at interfaces constituted by non-ionic molecules is still not fully understood. However, impurities or partial hydrolysis of monoolein can be safely ruled out in explaining the recorded negative  $\zeta$ -potential. Indeed, also cubosomes prepared using pure monoolein ( $> 99\%$ ) [31] or phytantriol[32] (a polar lipid that does not contain hydrolysable ester bonds) show high negative  $\zeta$ -potential. Rather, this fact may be justified assuming a hydroxide ions adsorption at the lipid/water interface originating a polarized outer layer surrounding the nanoparticles (a well-known phenomenon occurring at oil/water interfaces).[33,34] If this is correct, the substitution of the Pluronic with the PPE may play a fundamental role in a different hydroxide ions adsorption at the cubosome/water interface, and could be accounted for the increase of the  $\zeta$ -potential reported in Table 1.

Measurements of pH evidenced that formulations are slightly acidic, decreasing from pH = 6.50 (Cubo-0.3PPE) to pH = 6.27 (Cubo-1.2PPE) while increasing the PPE content (see Table S1). Remarkably, pH halved upon one-month aging in case of

cubosomes stabilized by the PPE, while it remained constant during this time frame when PF127 was used. Such a result is not surprising since PPE degradation originates phosphates that can provoke the detected drop of pH.

To understand how pH affects the physicochemical features of cubosomes stabilized by the new polyphosphoester polymer, the formulation Cubo-0.6PPE was diluted in two different buffers. PBS buffer at pH 7.4 (100 mM) and a citrate buffer at pH 3.4 (100 mM) were chosen to simulate the pH of a biological environment and the strong acidic character after one month of formulation ageing. Figure 3 summarizes the effect of pH on the cubosomes nanostructure. The initial pH of the formulation was 6.4 and the SAXS experiment revealed that cubosome nanostructure consisted solely of the cubic Pn3m phase. Whenever the sample is diluted in the PBS buffer (pH 7.4), no significant differences were noticed in comparison with the SAXS pattern at pH 6.4. Differently, when exposed to pH 3.4 the SAXS pattern evidenced the presence of both the Im3m and the Pn3m cubic bicontinuous phases (respectively showing lattice parameters of  $120.3 \pm 0.6$  and  $92.0 \pm 0.4$ , and water channel radii of  $19.7 \pm 0.2$  and  $19.0 \pm 0.2$ ). Due to the complex interaction of PPE with the lipid bilayer, the motivation for the inter-cubic phase transition at low pH was not fully understood, and requires further investigations. Contrarily, the internal phase of nanoparticles in Cubo-0.3F127 did not change when formulation was diluted with the citrate buffer at pH 3.4.

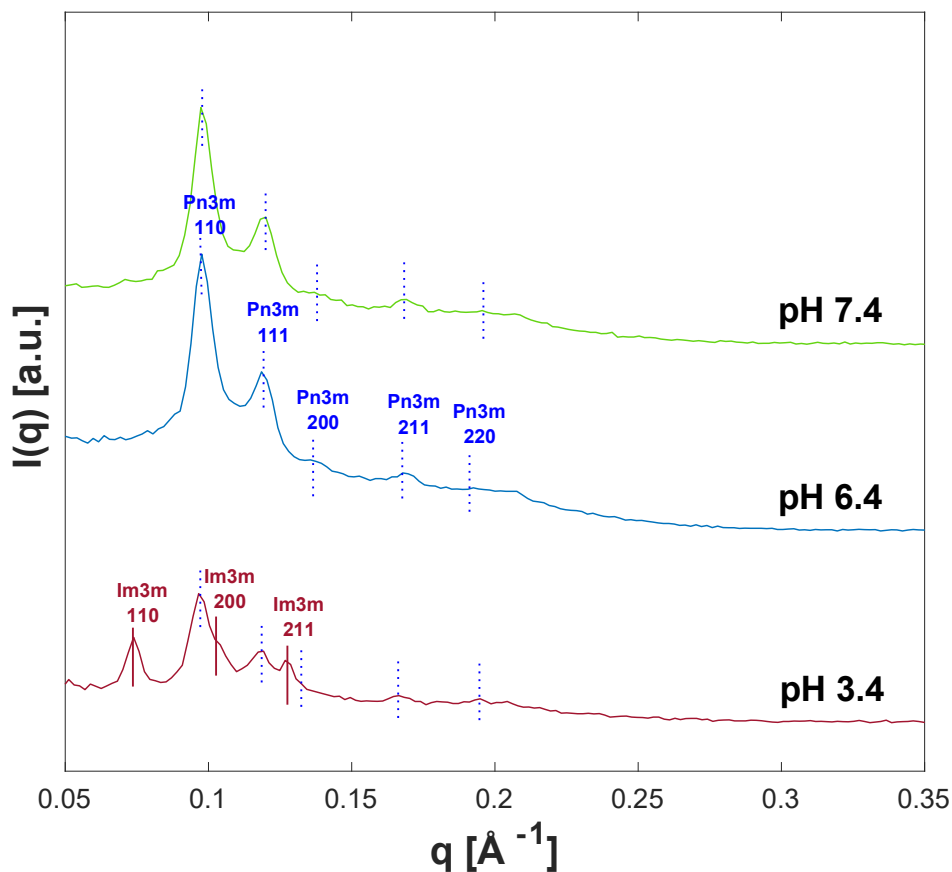


**Figure 3.** SAXS diffractograms at 25 °C of the formulation Cubo-0.6PPE at various pH.

The mean nanoparticles size in the Cubo-0.6PPE formulation did not vary significantly at the investigated pHs.  $D$  values of  $158.2 \pm 1.9$  (PDI =  $0.11 \pm 0.01$ ) and  $164.8 \pm 1.2$  (PDI =  $0.10 \pm 0.01$ ) were respectively found at pH 3.4 and 7.4. On the other hand, a drop in the  $\zeta$ -potential values was observed ( $-6.1 \pm 0.6$  and  $-10.2 \pm 0.8$  at pH 3.4 and 7.4, respectively), possibly due to the shielding effect caused by the presence of ions in the buffers.

Investigation of nanoparticle size, polydispersity index, and  $\zeta$ -potential over the time showed that only formulation Cubo-0.6PPE possesses good performances in terms of colloidal stability since no phase separation was noticed after more than 5 months (see Figure S3 a,b), while others formulations degraded after 4 weeks. Based on the stability

tests, further experiments were conducted only on formulation Cubo-0.6PPE. Particularly, the lyotropic behavior of the internal phase of the nanoparticles in formulation Cubo-0.6PPE was checked upon temperature change by SAXS (Figure 4).

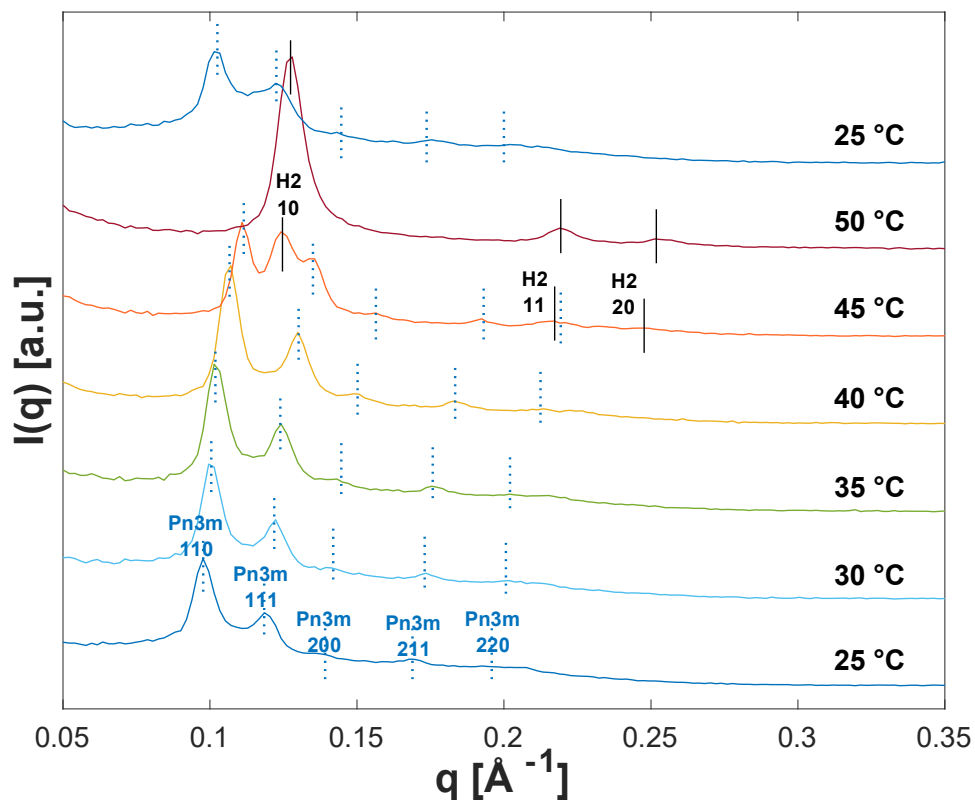


**Figure 4.** SAXS diffractograms of formulation Cubo-0.6PPE collected in the temperature range between 25 and 50 °C. On the top of the corresponding Bragg peaks, the Miller indices are also reported along with the indication of the phase.

**Table 2.** Phase, lattice parameter ( $a$ ), water channel radius ( $r_w$ ), of formulation Cubo-0.6PPE collected at different temperatures. Data at  $T = 25^*$  were calculated after cooling the sample down from 50 to 25 °C. Data are reported as mean  $\pm$  SD.

T (°C)	Phase	$a$ (Å)	$r_w$ (Å)
--------	-------	---------	-----------

25	Pn3m	91.2 ± 0.6	18.6 ± 0.1
30	Pn3m	89.1 ± 0.3	17.8 ± 0.1
35	Pn3m	87.9 ± 0.3	17.4 ± 0.1
40	Pn3m	83.9 ± 0.2	15.8 ± 0.1
45	Pn3m	80.4 ± 0.3	14.4 ± 0.1
	H <sub>2</sub>	57.1 ± 0.1	30.1 ± 0.2
50	H <sub>2</sub>	54.4 ± 3.2	29.4 ± 0.2
25*	Pn3m	90.8 ± 1.1	18.4 ± 0.4

In cubic bicontinuous liquid crystalline systems, the lipid hydrophobic chains become less ordered while increasing temperature,[30] thus provoking a more negative curvature of the lipid/water interface. Consequently, the lattice parameter of the cubosomes decreases as reported in Table 2. As shown in Figure 3, the Pn3m bicontinuous phase is retained up to 40 °C, while the diffraction pattern at 45 °C evidenced the simultaneous occurrence of a reverse hexagonal (H<sub>2</sub>) phase. The cubic-to-hexagonal phase transition at high temperature is a well-known phenomenon for MO-based liquid crystalline systems, but typically occurs at much higher temperature, around 90 °C according to the MO/W binary phase diagram.[35] However, it was established that the lyotropic behavior of dispersed cubic nanoparticles is different from that of the parent bulk phase. Specifically, experiments performed up to 95 °C on MO-based cubosomes dispersion stabilized with 1 wt % of PF127, demonstrated that the cubic-to-hexagonal transition do not occur.[36] Therefore, being the hydrophobic moiety of the PPE and PF127 polymers almost identical, the alteration of the cubosomes lyotropic behavior upon increasing the temperature here recorded could be

taken as a further evidence that the hydrophilic arms of the PPE strongly interact with the lipid interface. On the other hand, when the formulation was cooled down to ambient temperature, the Pn3m phase was reestablished, indicating the absence of hysteresis.

Since the cubosome formulation here under investigation is proposed as a drug carrier, the encapsulation of a hydrophobic payload was also studied. Quercetin, a hydrophobic natural antioxidant, was chosen as a drug model and its encapsulation was evaluated in Cubo-0.6PPE and, for the sake of comparison, in Cubo-0.3F127. After an excess of quercetin was added to the formulations, the latter were dialyzed to remove the non-encapsulated antioxidant.

The encapsulation efficiency was studied via UV-Vis spectroscopy after disruption of the formulation in EtOH, in which all the components of the dispersion are soluble. Cubo-0.3F127 and Cubo-0.6PPE presented the same EE% (respectively  $95.3 \pm 4.5$  and  $95.4 \pm 3.8$ ) and almost the same concentration of drug ( $(7.0 \pm 0.4) \times 10^{-4}$  M and  $(6.0 \pm 0.3) \times 10^{-4}$  M, respectively). This fact is not surprising, since the encapsulation of a hydrophobic drug basically depends on the amount of lipid used to prepare the formulation (identical in Cubo-0.3F127 and Cubo-0.6PPE).

### *3.3 In vitro toxicity studies*

A significant question of the current applications of cubosomes in medicine is the issue of safety. Although this is not a strong concern for preclinical studies using small animals, it is fundamental for the translation into clinical practice when the toxicity of these bicontinuous cubic liquid crystalline nanoparticles needs to be carefully evaluated. It was previously speculated that MO, a membrane lipid, could promote bio-adhesion and internalization of PF127, which is used to stabilize the formulation. After



passage through the cell membrane, PF127 inevitably ends up in contact with the intracellular space and could induce damage toward mitochondrial and nuclear membranes, leading to cell death.[37] Therefore, the rationale behind replacing PF127 with PPE to stabilize the formulation is the reduced exposure of intracellular space to toxic agents.

Nowadays, biological aspects of interactions between cubosomes and cells are becoming less and less obscure, and experimental evidence showed that cytotoxicity differed significantly in their response *in vitro*, depending on the cellular line investigated.[38–40] The present study aimed to compare the cytotoxicity of PF127-(Cubo-0.3F127) and PPE-stabilized (Cubo-0.6PPE) MO-based cubosomes after exposure to two different cell lines. The concentrations chosen encompassed the range at which cytogenotoxic responses were previously observed and taken into consideration the expected medical applications *in vivo*. Indeed, previous *in vivo* studies on this kind of nanoparticles stabilized by Pluronic F108 showed that a MO concentration lower than 60 µg per mL of plasma is required to prevent hemolysis.[41] Figure 5 shows the cell viability of a HEK-293 cell line after the treatment with all the formulations here under investigation. Cytotoxicity was evaluated by an assay measuring changes in membrane integrity that occur as a result of cell death. The viability analysis displayed the highest cytotoxic activity in the cells treated with formulation Cubo-0.3F127 with respect to formulation Cubo-0.6PPE. There is no loss of cell viability up to 50 µg/mL, and this value is in line with other studies that analyzed the toxicity of MO-based cubosomes with the Hek293 cell line.

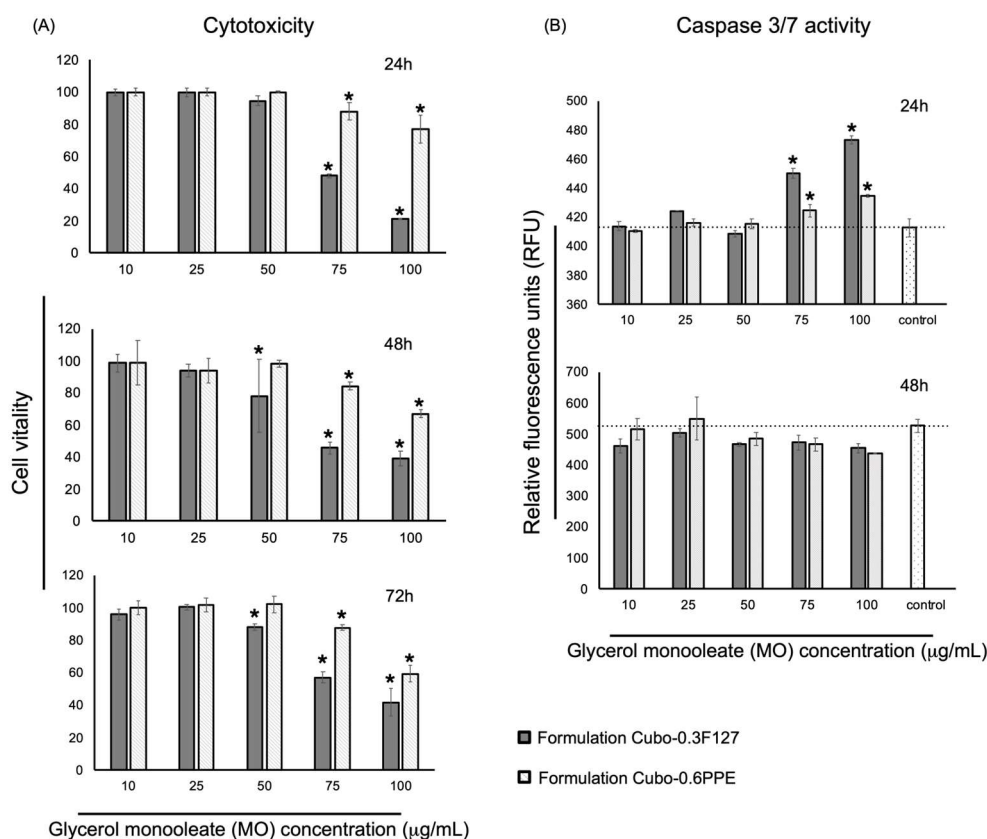


**Figure 5.** (A) Cellular viability of Human Embryonic Kidney (HEK) 293 cells incubated with formulations Cubo-0.3F127 and Cubo-0.6PPE at different concentrations for 24, 48, and 72 h. Data are shown as mean  $\pm$  SD of 3 individual experiments. (B) Effects on caspase 3/7 activity in HEK-293 cells induced by treatment with formulations Cubo-0.3F127 and Cubo-0.6PPE. Enzymatic activities of caspase 3/7 after 24 and 48 h treatment of HEK-293 cells with medium as control, formulations Cubo-0.3F127 and Cubo-0.6PPE at different concentrations. The caspase activity is expressed as the relative fluorescence unit (RFU), measured after 30 minutes by the Glomax MultiDetection System instrument (Promega Madison, WI). \* $P < 0.05$ .

The induction of cytotoxicity after the exposure at a higher concentration was particularly marked with formulation Cubo-0.3F127 (Figure 5A). Along with the loss of cell viability, it was noted a significant increase in the caspase 3/7 activity in the cells

treated with formulation Cubo-0.3F127 compared to formulation Cubo-0.6PPE. These studies revealed an intriguing feature: the HEK-293 cell line increased their caspase 3/7 activity in a transient manner (24 h) after the exposure at higher concentrations. Indeed, it was not observed any effect on caspase 3/7 activity at longer exposure time (Figure 5B).

Besides, it was detected that the formulation Cubo-0.3F127 exposure induced significant cytotoxicity in the HUVECs cell line at the highest concentration (100  $\mu\text{g}/\text{mL}$ ), whereas when formulation Cubo-0.6PPE was used the HUVECs viability (Figure 6A) was not affected. It deserves noticing that, apparently, Cubo-0.3F127 at a concentration of 100  $\mu\text{g}/\text{mL}$  was less cytotoxic after 48 h rather than 24 h cell treatment. It can be speculated that this finding is related to the uptake of nanoparticles, and their persistence at cellular level. Understanding of the toxicity mechanism will require further investigation. Of interest, formulation Cubo-0.3F127 induced a significant increase in the caspase 3/7 activity after 24 h of exposure compared to formulation Cubo-0.6PPE as previously described for the HEK-293 cells (Figure 6B). In parallel, the cellular morphology of HUVECs was examined through fluorescence microscopy. The effects of Cubo-0.3F127 on cell morphology were consistent with their reported ability to cause cell death (Figure 6C).

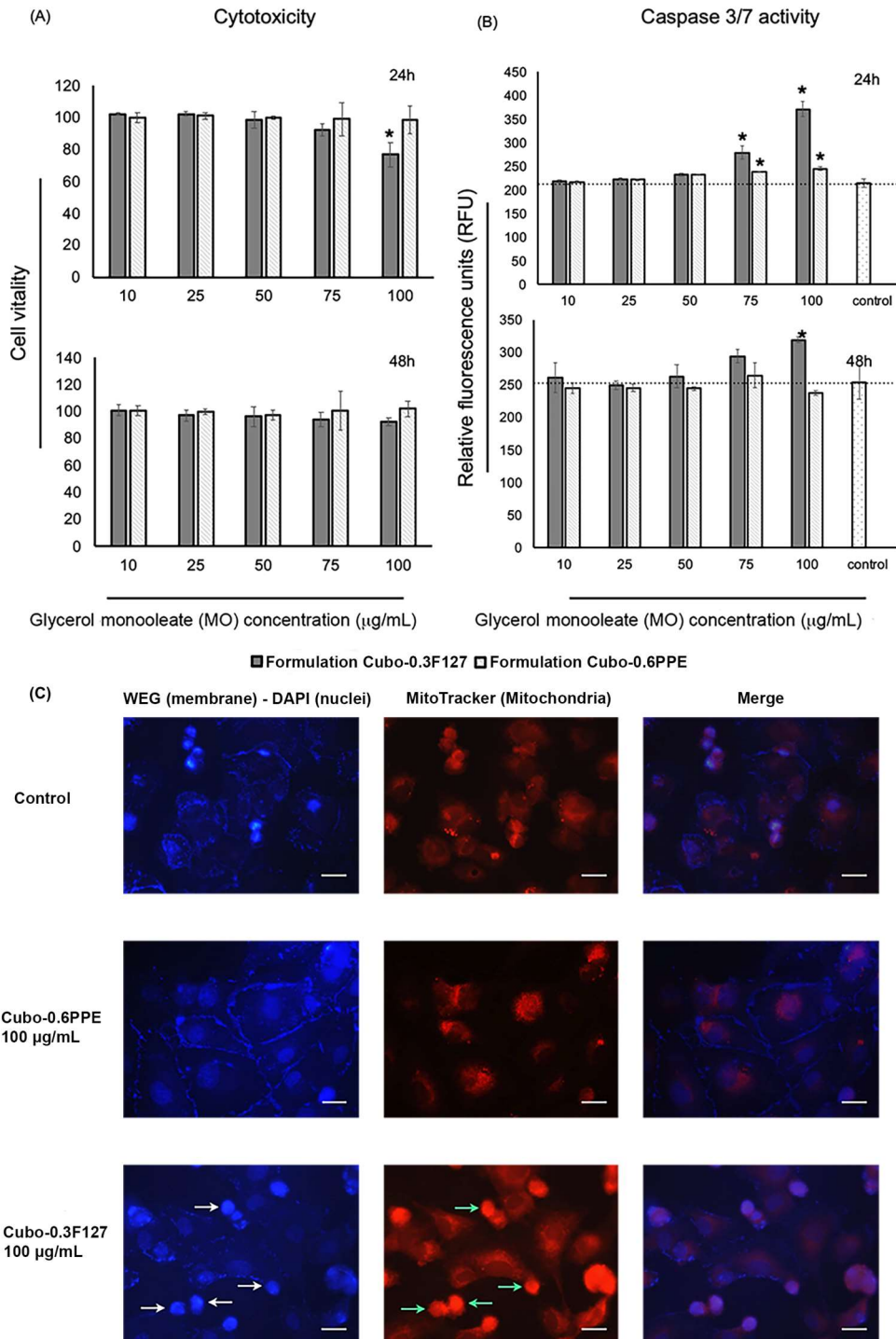


**Figure 6.** (A) Cellular viability of Human Umbilical Vein Embryonic Cells (HUVECs) incubated with formulations Cubo-0.3F127 and Cubo-0.6PPE at different concentrations for 24 and 48 h. Data are shown as mean  $\pm$  SD of 3 individual experiments. (B) Effects on caspase 3/7 activity in HUVECs cells induced by treatment

with formulations Cubo-0.3F127 and Cubo-0.6PPE. Enzymatic activities of caspase 3/7 after 24- and 48-hours treatment of HUVECs cells with medium as control, formulations Cubo-0.3F127 and Cubo-0.6PPE at different concentrations. The caspase activity is expressed as the relative fluorescence unit (RFU), measured after 30 minutes by the Glomax MultiDetection System instrument (Promega Madison, WI). \* $P < 0.05$ .

(C) Fluorescence microscopy images. HUVECs were incubated for 24 hours in medium alone (control) or in presence of formulations Cubo-0.3F127 or Cubo-0.6PPE at the MO concentration of 100  $\mu\text{g}/\text{mL}$ . Cells were subsequently fixed and stained with MitoTracker (mitochondria, red), Wheat Germ Agglutinin (WGA) derivative (membranes, blue) and DAPI (nuclei, blue). Cubo-0.3F127 treated sample contains a number of cells characterized by condensed nuclei. Fluorescent mitochondria images can be correlated with nuclear phenomena made evident by DAPI staining: white arrows indicate the nuclei, and green arrows the co-localized mitochondria. Effects of Cubo-0.3F127 on morphology are consistent with their reported ability to cause cell death. Bar = 50 nm.

After the general cytotoxic evaluation of our formulation Cubo-0.3F127 and Cubo-0.6PPE, we performed a hemolysis assay that we conceived as a proof-of-concept to preliminarily assess (*in vitro*) hemocompatibility of the new nanocarriers. As can be seen in Figure 7, it is noteworthy that in samples treated with formulation Cubo-0.6PPE, the percentage of hemolysis rate was lower than the 5% allowed according to ISO/TR 7406 (samples with a hemolytic ratio of less than 5% are considered nonhemolytic) up to MO concentration of 50  $\mu\text{g}/\text{mL}$ . Overall, we observed the presence of significant amounts of hemoglobin in the supernatant of samples treated with formulation Cubo-0.3F127 compared to formulation Cubo-0.6PPE. These features may contribute to

improving the drawbacks of conventional cubosomes formulations, and therefore will require further investigations.

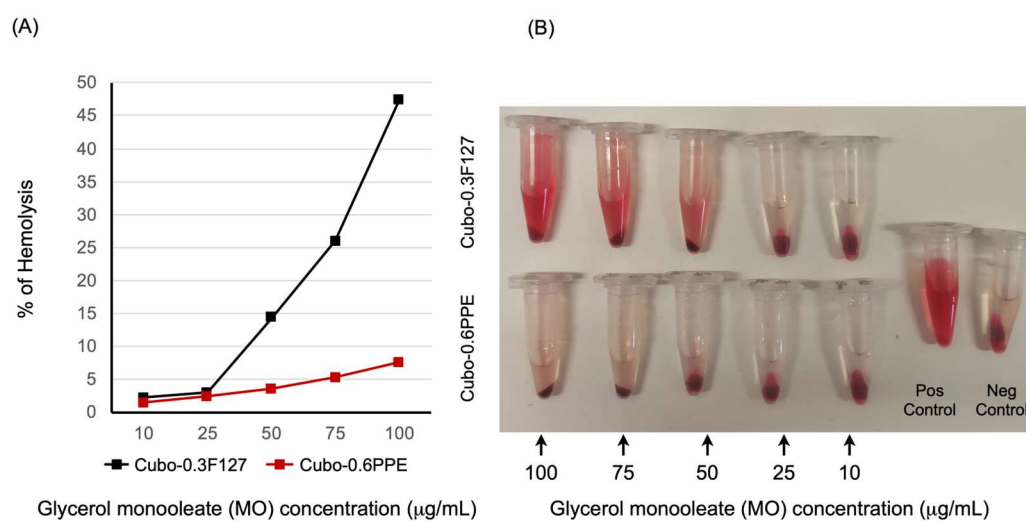


**Figure 7.** Hemolysis assay on formulation Cubo-0.3F127 and Cubo-0.6PPE. (A) Relative rate of hemolysis in human erythrocytes following 1 h incubation with different concentrations of formulation Cubo-0.3F127 and Cubo-0.6PPE at 37 °C. (B) Photograph of fresh human blood incubated with different concentrations of formulation Cubo-0.3F127 and Cubo-0.6PPE after centrifugation at 10000 rpm for 5 min. Saline solution (0.9 % NaCl) and distilled water were employed respectively as the negative control (0 % lysis) and positive control (100 % lysis). Error bars in (A) are not reported since the standard deviations of triplicate data points of absorbance reading are negligible.

The capacity to limit the activation of the complement system is another pivotal characteristic of nanostructures;[42,43] in fact, deposition of complement components on their surface induce particle degradation and fast elimination caused by enhanced phagocytosis. Formulations Cubo-0.3F127 or Cubo-0.6PPE (660 µg/mL) have been

incubated with human serum for 2 hours at 37 °C. The residual activity of the complement system was measured using a hemolytic assay rather than the quantification of activation products by ELISA.[16] Indeed, quantification of the complement activation products C5a and C5b-9 by ELISA is often used to evaluate capacity of the nanoparticles to activate the complement system. However, this analysis can be influenced by the amount of molecules adsorbed on the nanoparticles surface, while the residual activity is not. Cubo-0.3F127 activates and partially consumes the complement system in human serum, reducing to about 60 % of the residual activity. On the contrary, Cubo-0.6PPE preparation seems to slightly interact with the complement system and residual activity remains over 90 % (Figure 8).

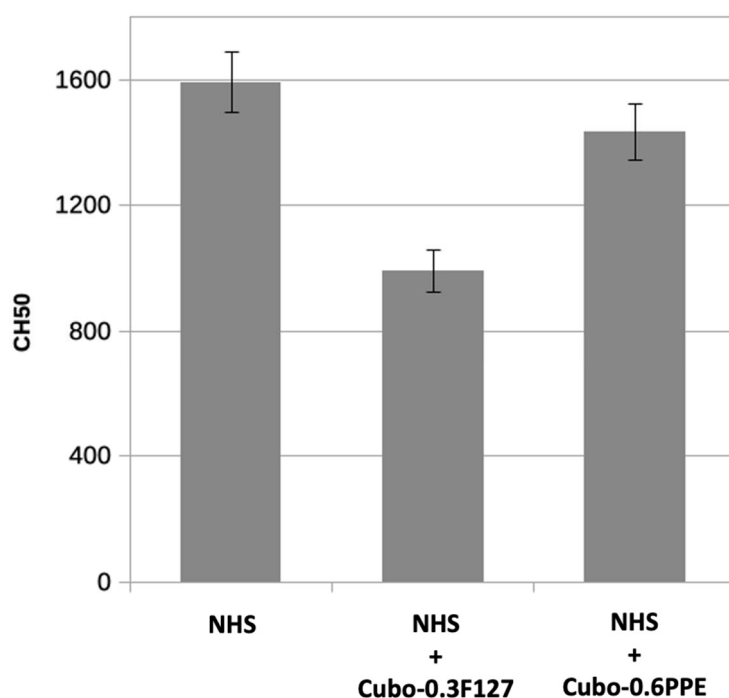


**Figure 8.** Activation of the complement system in normal human serum (NHS) by formulation Cubo-0.3F127 and Cubo-0.6PPE. Residual activity of the complement system in human serum incubated with formulation Cubo-0.3F127 and Cubo-0.6PPE for 2 h at 37 °C was measured using a hemolytic test. Data (mean +/- SD) are expressed as CH50, calculated as the amount (in nL) of treated serum required to induce 50 % of

*red blood cell lysis in the test. NHS vs (NHS + Cubo-0.3F127) showed  $p < 0.01$  while NHS vs (NHS + Cubo-0.6PPE) showed no statistical difference.*

#### **4. Conclusions**

Nanocarrier cytotoxicity represents one of the most important complications that researchers working in the field of drug delivery have to solve. In the case of cubosomes, such toxicity is exerted mainly towards erythrocytes, as pointed out by several studies.[44,45] To overcome this issue, increasing the cubosomes biocompatibility in general, and with particular reference to their hemocompatibility, a newly synthesized poly-(phosphoester) structurally analog of the traditional PF127, was used to stabilize these nanoparticles dispersion in water. According to the physicochemical experiments here discussed, the PPE effectively stabilized the dispersion against flocculation while preserving the original nanostructure expected for the self-assembly of monoolein in excess of water. In comparison with PF127-cubosomes, *in vitro* toxicity studies on two different cell lines (HEK-293 and HUVEC) and human erythrocytes proved the higher biocompatibility of PPE-cubosomes and, remarkably, their excellent hemocompatibility. In serum, the capacity to trigger the complement system was particularly high in formulation Cubo-0.3F127, possibly activating the alternative pathway of the complement system, through the binding and the activation of the complement component C3.[46] On the contrary, formulation Cubo-0.6PPE apparently does not interact with C3 and avoids the typical nucleophilic attack of C3. In conclusion, the reduced capacity of activating the complement system guarantee increased stability and biocompatibility and a lower elimination by phagocytes. It is worth recalling that when in contact with biological fluids such as blood plasma or serum, lyotropic liquid crystalline nanoparticles, (which includes



cubosomes and hexosomes, among others) may undergo structural alterations or, in some cases, phase transition. Such aspect, not investigated here, was recently reviewed in detail.[39]

Nature and living cells employ several PPEs-based structures, given the high stability of the C-O-P bond. Nevertheless, this bond is degradable on demand through specific enzymes,[47,48] depending on factors such as the polymer architecture and its hydrophilicity.[49] On the other hand, PEO-based polymers (i.e. PEG and Pluronic F127) are not a biodegradable and their accumulation inside cells can lead to a cytotoxic effect.[50] For the desired application in nanomedicine, the choice of using PPEs instead of Pluronics as a stabilizer for lyotropic liquid crystalline nanoparticles (such as cubosomes) could avoid the side effects in terms of cytotoxicity, given its intrinsic biodegradability.

Taking into account the possibility of synthesizing polyphosphoesters able to properly stabilize cubosomes also conjugated with imaging or targeting probes, results discussed in this paper pave the way for the development of a new generation of more biocompatible bicontinuous cubic liquid crystalline nanoparticles useful for a wide range of nanomedicine applications.

## **Acknowledgments**

Prof. Tommy Nylander and Prof. Karin Schillén are kindly thanked for precious discussions and suggestions. The authors would like to thank Dr. Anna Karnerup for the precious help for cryo-TEM measurements. SM thanks Fondazione Banco di Sardegna and Regione Autonoma della Sardegna (Progetti Biennali di Ateneo

Annualità 2018). MF thanks P.O.R. Sardegna F.S.E. 2014-2020 for funding his Ph.D. Scholarship.

## References

- [1] G. Chen, I. Roy, C. Yang, P.N. Prasad, Nanochemistry and Nanomedicine for Nanoparticle-based Diagnostics and Therapy, *Chem. Rev.* 116 (2016) 2826–2885. doi:10.1021/acs.chemrev.5b00148.
- [2] J.K. Fard, S. Jafari, M.A. Eghbal, A review of molecular mechanisms involved in toxicity of nanoparticles, *Adv. Pharm. Bull.* 5 (2015) 447–454. doi:10.15171/apb.2015.061.
- [3] A.C. Anselmo, S. Mitragotri, Nanoparticles in the clinic: An update, *Bioeng. Transl. Med.* 4 (2019) 1–16. doi:10.1002/btm2.10143.
- [4] J. Wolfram, M. Ferrari, Clinical cancer nanomedicine, *Nano Today.* 25 (2019) 85–98. doi:10.1016/j.nantod.2019.02.005.
- [5] J.A. Barreto, W. O'Malley, M. Kubeil, B. Graham, H. Stephan, L. Spiccia, Nanomaterials: Applications in Cancer Imaging and Therapy, *Adv. Mater.* 23 (2011) H18–H40. doi:10.1002/adma.201100140.
- [6] J. Zhai, C. Fong, N. Tran, C.J. Drummond, Non-Lamellar Lyotropic Liquid Crystalline Lipid Nanoparticles for the Next Generation of Nanomedicine, *ACS Nano.* (2019). doi:10.1021/acsnano.8b07961.
- [7] R. Mezzenga, J.M. Seddon, C.J. Drummond, B.J. Boyd, G.E. Schröder-Turk, L. Sagalowicz, Nature-Inspired Design and Application of Lipidic Lyotropic Liquid Crystals, *Adv. Mater.* 31 (2019) 1–19. doi:10.1002/adma.201900818.
- [8] H.M.G. Barriga, M.N. Holme, M.M. Stevens, Cubosomes: The Next Generation of Smart Lipid Nanoparticles?, *Angew. Chemie - Int. Ed.* 58 (2019)

- 2958–2978. doi:10.1002/anie.201804067.
- [9] S. Murgia, S. Biffi, R. Mezzenga, Recent advances of non-lamellar lyotropic liquid crystalline nanoparticles in nanomedicine, *Curr. Opin. Colloid Interface Sci.* 48 (2020) 28–39. doi:10.1016/j.cocis.2020.03.006.
- [10] J.A. Prange, S. Aleandri, M. KomisarSKI, A. Luciani, A. Käch, C.D. Schuh, et al., Overcoming Endocytosis Deficiency by Cubosome Nanocarriers, *ACS Appl. Bio Mater.* 2 (2019) 2490–2499. doi:10.1021/acsabm.9b00187.
- [11] V. Meli, C. Caltagirone, A.M. Falchi, S.T. Hyde, V. Lippolis, M. Monduzzi, et al., Docetaxel-Loaded Fluorescent Liquid-Crystalline Nanoparticles for Cancer Theranostics, *Langmuir.* 31 (2015) 9566–9575. doi:10.1021/acs.langmuir.5b02101.
- [12] A.M. Bodratti, P. Alexandridis, Formulation of poloxamers for drug delivery, *J. Funct. Biomater.* 9 (2018). doi:10.3390/jfb9010011.
- [13] E. Tasca, A. Del Giudice, L. Galantini, K. Schillén, A.M. Giuliani, M. Giustini, A fluorescence study of the loading and time stability of doxorubicin in sodium cholate/PEO-PPO-PEO triblock copolymer mixed micelles, *J. Colloid Interface Sci.* 540 (2019) 593–601. doi:10.1016/j.jcis.2019.01.075.
- [14] E. V. Batrakova, A. V. Kabanov, Pluronic block copolymers: Evolution of drug delivery concept from inert nanocarriers to biological response modifiers, *J. Control. Release.* 130 (2008) 98–106. doi:10.1016/j.jconrel.2008.04.013.
- [15] S. Bayati, L. Galantini, K.D. Knudsen, K. Schillén, Effects of Bile Salt Sodium Glycodeoxycholate on the Self-Assembly of PEO-PPO-PEO Triblock Copolymer P123 in Aqueous Solution, *Langmuir.* 31 (2015) 13519–13527. doi:10.1021/acs.langmuir.5b03828.
- [16] I.D.M. Azmi, P.P. Wibroe, L.P. Wu, A.I. Kazem, H. Amenitsch, S.M.

- Moghimi, et al., A structurally diverse library of safe-by-design citrem-phospholipid lamellar and non-lamellar liquid crystalline nano-assemblies, *J. Control. Release.* 239 (2016) 1–9. doi:10.1016/j.jconrel.2016.08.011.
- [17] J.Y.T. Chong, X. Mulet, A. Postma, D.J. Keddie, L.J. Waddington, B.J. Boyd, et al., Novel RAFT amphiphilic brush copolymer steric stabilisers for cubosomes: poly(octadecyl acrylate)-block-poly(polyethylene glycol methyl ether acrylate)., *Soft Matter.* 10 (2014) 6666–6676. doi:10.1039/c4sm01064g.
- [18] M. Johnsson, J. Barauskas, A. Norlin, F. Tiberg, Physicochemical and Drug Delivery Aspects of Lipid-Based Liquid Crystalline Nanoparticles: A Case Study of Intravenously Administered Propofol, *J. Nanosci. Nanotechnol.* 6 (2006) 3017–3024. doi:10.1166/jnn.2006.402.
- [19] J.Y.T. Chong, X. Mulet, D.J. Keddie, L. Waddington, S.T. Mudie, B.J. Boyd, et al., Novel Steric Stabilizers for Lyotropic Liquid Crystalline Nanoparticles: PEGylated-Phytanyl Copolymers, *Langmuir.* 31 (2015) 2615–2629. doi:10.1021/la501471z.
- [20] J.L. Grace, N. Alcaraz, N.P. Truong, T.P. Davis, B.J. Boyd, J.F. Quinn, et al., Lipidated polymers for the stabilization of cubosomes: Nanostructured drug delivery vehicles, *Chem. Commun.* 53 (2017) 10552–10555. doi:10.1039/c7cc05842j.
- [21] J. Zhai, T.M. Hinton, L.J. Waddington, C. Fong, N. Tran, X. Mulet, et al., Lipid-PEG Conjugates Sterically Stabilize and Reduce the Toxicity of Phytantriol-Based Lyotropic Liquid Crystalline Nanoparticles., *Langmuir.* 31 (2015) 10871–10880. doi:10.1021/acs.langmuir.5b02797.
- [22] J. Zhai, R. Suryadinata, B. Luan, N. Tran, T.M. Hinton, J. Ratcliffe, et al., Amphiphilic brush polymers produced using the RAFT polymerisation method

- stabilise and reduce the cell cytotoxicity of lipid lyotropic liquid crystalline nanoparticles., *Faraday Discuss.* (2016) Ahead of Print.  
doi:10.1039/C6FD00039H.
- [23] T. Steinbach, F.R. Wurm, Poly(phosphoester)s: A New Platform for Degradable Polymers, *Angew. Chemie - Int. Ed.* 54 (2015) 6098–6108.  
doi:10.1002/anie.201500147.
- [24] M. Worm, B. Kang, C. Dingels, F.R. Wurm, H. Frey, *Macromolecular Rapid Communications* Acid-labile Amphiphilic PEO- b -PPO- b -PEO Copolymers : Degradable Poloxamer Analogs, (n.d.) 775–780.
- [25] J. Simon, K.N. Bauer, J. Langhanki, T. Opatz, V. Mailänder, K. Landfester, et al., Noncovalent Targeting of Nanocarriers to Immune Cells with Polyphosphoester-Based Surfactants in Human Blood Plasma, *Adv. Sci.* 6 (2019). doi:10.1002/advs.201901199.
- [26] B. Clément, B. Grignard, L. Koole, C. Jérôme, P. Lecomte, Metal-free strategies for the synthesis of functional and well-defined polyphosphoesters, *Macromolecules.* 45 (2012) 4476–4486. doi:10.1021/ma3004339.
- [27] L. Mazzarino, G. Loch-Neckel, L. dos S. Bubniak, F. Ourique, I. Otsuka, S. Halila, et al., Nanoparticles made from xyloglucan-block-polycaprolactone copolymers: Safety assessment for drug delivery, *Toxicol. Sci.* 147 (2015) 104–115. doi:10.1093/toxsci/kfv114.
- [28] R. Marzari, D. Sblattero, P. Macor, F. Fischetti, R. Gennaro, J.D. Marks, et al., The cleavage site of C5 from man and animals as a common target for neutralizing human monoclonal antibodies: In vitro and in vivo studies, *Eur. J. Immunol.* 32 (2002) 2773–2782. doi:10.1002/1521-4141(2002010)32:10<2773::AID-IMMU2773>3.0.CO;2-G.

- [29] D. Demurtas, P. Guichard, I. Martiel, R. Mezzenga, C. Hebert, L. Sagalowicz, Direct visualization of dispersed lipid bicontinuous cubic phases by cryo-electron tomography., *Nat. Commun.* 6 (2015) 8915.  
doi:10.1038/ncomms9915.
- [30] M. Nakano, A. Sugita, H. Matsuoka, T. Handa, Small-angle X-ray scattering and <sup>13</sup>C NMR investigation on the internal structure of “Cubosomes,” *Langmuir*. 17 (2001) 3917–3922. doi:10.1021/la010224a.
- [31] S. Murgia, A.M. Falchi, V. Meli, K. Schillén, V. Lippolis, M. Monduzzi, et al., Cubosome formulations stabilized by a dansyl-conjugated block copolymer for possible nanomedicine applications, *Colloids Surfaces B Biointerfaces*. 129 (2015) 87–94. doi:10.1016/j.colsurfb.2015.03.025.
- [32] S.P. Akhlaghi, I.R. Ribeiro, B.J. Boyd, W. Loh, Impact of preparation method and variables on the internal structure, morphology, and presence of liposomes in phytantriol-Pluronic® F127 cubosomes, *Colloids Surfaces B Biointerfaces*. 145 (2016) 845–853. doi:10.1016/j.colsurfb.2016.05.091.
- [33] J.K. Beattie, A.M. Djerdjev, The pristine oil/water interface: Surfactant-free hydroxide-charged emulsions, *Angew. Chemie - Int. Ed.* 43 (2004) 3568–3571.  
doi:10.1002/anie.200453916.
- [34] C.D. Driever, X. Mulet, L.J. Waddington, A. Postma, H. Thissen, F. Caruso, et al., Layer-by-layer polymer coating on discrete particles of cubic lyotropic liquid crystalline dispersions (cubosomes), *Langmuir*. 29 (2013) 12891–12900.  
doi:10.1021/la401660h.
- [35] H. Qiu, M. Caffrey, The phase diagram of the monoolein/water system: Metastability and equilibrium aspects, *Biomaterials*. 21 (2000) 223–234.  
doi:10.1016/S0142-9612(99)00126-X.

- [36] Y. Da Dong, A.J. Tilley, I. Larson, M. Jayne Lawrence, H. Amenitsch, M. Rappolt, et al., Nonequilibrium effects in self-assembled mesophase materials: Unexpected supercooling effects for cubosomes and hexosomes, *Langmuir*. 26 (2010) 9000–9010. doi:10.1021/la904803c.
- [37] S. Murgia, A.M. Falchi, M. Mano, S. Lampis, R. Angius, A.M. Carnerup, et al., Nanoparticles from lipid-based liquid crystals: Emulsifier influence on morphology and cytotoxicity, *J. Phys. Chem. B*. 114 (2010). doi:10.1021/jp9098655.
- [38] A.M. Falchi, A. Rosa, A. Atzeri, A. Incani, S. Lampis, V. Meli, et al., Effects of monoolein-based cubosome formulations on lipid droplets and mitochondria of HeLa cells, *Toxicol. Res. (Camb)*. 4 (2015). doi:10.1039/c5tx00078e.
- [39] A. Tan, L. Hong, J.D. Du, B.J. Boyd, Self-Assembled Nanostructured Lipid Systems: Is There a Link between Structure and Cytotoxicity?, *Adv. Sci*. 6 (2019) 1801223. doi:10.1002/advs.201801223.
- [40] A. Rosa, S. Murgia, D. Putzu, V. Meli, A.M. Falchi, Monoolein-based cubosomes affect lipid profile in HeLa cells, *Chem. Phys. Lipids*. 191 (2015) 96–105. doi:10.1016/j.chemphyslip.2015.08.017.
- [41] S. Biffi, L. Andolfi, C. Caltagirone, C. Garrovo, A.M. Falchi, V. Lippolis, et al., Cubosomes for in vivo fluorescence lifetime imaging, *Nanotechnology*. 28 (2017). doi:10.1088/1361-6528/28/5/055102.
- [42] P.P. Wibroe, I.D. Mat Azmi, C. Nilsson, A. Yaghmur, S.M. Moghimi, Citrem modulates internal nanostructure of glyceryl monooleate dispersions and bypasses complement activation: Towards development of safe tunable intravenous lipid nanocarriers, *Nanomedicine Nanotechnology, Biol. Med*. 11 (2015) 1909–1914. doi:10.1016/j.nano.2015.08.003.

- [43] I.D. Mat Azmi, L. Wu, P.P. Wibroe, C. Nilsson, J. Østergaard, S. Stürup, et al., Modulatory Effect of Human Plasma on the Internal Nanostructure and Size Characteristics of Liquid-Crystalline Nanocarriers, *Langmuir*. 31 (2015) 5042–5049. doi:10.1021/acs.langmuir.5b00830.
- [44] J. Barauskas, C. Cervin, M. Jankunec, M. Špandyreva, K. Ribokaitė, F. Tiberg, et al., Interactions of lipid-based liquid crystalline nanoparticles with model and cell membranes, *Int. J. Pharm.* 391 (2010) 284–291. doi:10.1016/j.ijpharm.2010.03.016.
- [45] J.C. Bode, J. Kuntsche, S.S. Funari, H. Bunjes, Interaction of dispersed cubic phases with blood components., *Int. J. Pharm.* 448 (2013) 87–95. doi:10.1016/j.ijpharm.2013.03.016.
- [46] K. Yu, B.F.L. Lai, J.H. Foley, M.J. Krisinger, E.M. Conway, J.N. Kizhakkedathu, Modulation of complement activation and amplification on nanoparticle surfaces by glycopolymer conformation and chemistry, *ACS Nano*. 8 (2014) 7687–7703. doi:10.1021/nn504186b.
- [47] D.F. Xiang, A.N. Bigley, Z. Ren, H. Xue, K.G. Hull, D. Romo, et al., Interrogation of the Substrate Profile and Catalytic Properties of the Phosphotriesterase from *Sphingobium* sp. Strain TCM1: An Enzyme Capable of Hydrolyzing Organophosphate Flame Retardants and Plasticizers, *Biochemistry*. 54 (2015) 7539–7549. doi:10.1021/acs.biochem.5b01144.
- [48] Y.C. Wang, L.Y. Tang, T.M. Sun, C.H. Li, M.H. Xiong, J. Wang, Self-assembled micelles of biodegradable triblock copolymers based on poly(ethyl ethylene phosphate) and poly( $\epsilon$ -caprolactone) as drug carriers, *Biomacromolecules*. 9 (2008) 388–395. doi:10.1021/bm700732g.
- [49] K.N. Bauer, H.T. Tee, M.M. Velencoso, F.R. Wurm, Main-chain



poly(phosphoester)s: History, syntheses, degradation, bio-and flame-retardant applications, *Prog. Polym. Sci.* 73 (2017) 61–122.

doi:10.1016/j.progpolymsci.2017.05.004.

- [50] S. Schöttler, G. Becker, S. Winzen, T. Steinbach, K. Mohr, K. Landfester, et al., Protein adsorption is required for stealth effect of poly(ethylene glycol)- and poly(phosphoester)-coated nanocarriers, *Nat. Nanotechnol.* 11 (2016) 372–377. doi:10.1038/nnano.2015.330.

## Graphical Abstract

